ChemComm

ROYAL SOCIETY OF CHEMISTRY

COMMUNICATION

View Article Online
View Journal | View Issue

Check for updates

Cite this: *Chem. Commun.*, 2021, **57**, 5020

Received 8th March 2021,
Accepted 14th April 2021

DOI: 10.1039/d1cc01249e

rsc.li/chemcomm

Chiral induction in boron imidazolate frameworks: the construction of cage-based absolute helices†

Ming-Yue Bi,[a] Qin-Long Hong,[a] Meng Liu,[b] Fei Wang,[a] Hai-Xia Zhang*[a] and Jian Zhang*[a]

Two cage-based boron imidazolate helices were prepared in achiral reaction systems by mixing a C_3 symmetric rigid ligand, KBH(bim)$_3$, and a long flexible dicarboxylic acid ligand. The presence of an appropriate chiral inducer can control the helical orientation of bulk samples, which further acts on the enantioselective separation of racemic 1-phenylethanol.

Chirality is one of the essential features in organic life to perform a series of complicated biological functions, especially in biopolymers such as nucleic acids and DNA, in which the helix is one of the most important states.[1–5] Homochirality and helicity are also common in inorganic minerals, as evidenced by the ubiquity of calcite and quartz.[6] It has even been speculated that biological homochirality may originate from interactions with abundant inorganic minerals.[7] Recently, metal–organic frameworks (MOFs), a family of hybrid organic–inorganic coordination materials, have received great attention because of their incorporation of functionality from both inorganic and organic components.[8–15] In particular, the construction of homochiral MOFs may help to provide new opportunities for better understanding the origin of biological homochirality.[16–24] Various synthetic approaches have been pursued and developed for fabricating homochiral MOFs from enantiopure or achiral ligands.[25–28] However, the investigation of 1-dimensional (1-D) metal–organic helical chains with only the axes symmetry and their enantioselective separation remain little explored.[29,30]

Mimicking the helical features of biopolymers such as DNA in the organic–inorganic hybrid way is of great significance to elucidate the interactions between the origin of biological homochirality and the inorganic nature. Chirality can be expressed at different levels, including molecular chirality (such as chiral carbon centers) and spatial chirality (formed from the spatial organization of molecular building blocks, such as helical conformation).[6] Biopolymeric helicity is a special 1-D chirality, which displays dual homochiral features with both molecular chirality and spatial chirality. The handedness of the biopolymeric helix can be precisely controlled, such as D-sugars leads to the right-handed helicity. Unlike biopolymers, inorganic minerals, such as quartz, formed from the spatial organization of achiral precursors and intertwined helices are generated and stabilized in a 3-D net; such organization usually results in the formation of both right- and left-handed forms.[7] Since MOFs can integrate both molecular chirality and absolute helicity, both types of helices can be fabricated from chiral or achiral precursor.[31–35] However, no matter which precursor is used, the formed helices only act as a part of the whole network being embedded or hosted in the 3-D MOF, which is similar to the assembly mode of inorganic materials and unlike that of polymeric DNA. The isolation and stabilization of the 1-D absolute helix and controlling its handedness still remain a big challenge.[36]

Therefore, our aim is to develop a strategic approach to synthesize absolute helix by the self-assembly of metal-ions and organic ligands. The combination of a C_3 symmetric rigid ligand, KBH(bim)$_3$, (bim = benzimidazole) and a long flexible dicarboxylic acid ligand is chosen to construct the helical chains. Herein, two homochiral boron imidazolate frameworks (BIFs) with the absolute helicity structures $Zn_4[BH(bim)_3]_4(obb)(H_2O)_2\cdot(NO_3)_2$ (BIF-109-Zn, obb = 4,4′-oxybis(benzoate)) and $Zn_4[BH(bim)_3]_4(cdba)(H_2O)_2\cdot(NO_3)_2$ (BIF-110-Zn, cdba = 4,4′-carbonyldibenzoic acid) were successfully synthesized and structurally characterized. Interestingly, the bulk homochiral crystals of BIF-109-Zn (M) and BIF-109-Zn (P) can be obtained in the presence of proper chiral induction agents. The as-obtained BIF-109-Zn (M) crystals exhibited enantioselective separation of racemic 1-phenylethanol with an enantiomeric excess (ee) value of 72%.

---

[a] *State Key Laboratory of Structural Chemistry, Fujian Institute of Research on the Structure of Matter, Chinese Academy of Sciences, Fuzhou, Fujian 350002, P. R. China. E-mail: zhanghaixia@fjirsm.ac.cn, zhj@fjirsm.ac.cn*

[b] *Key Lab for Sport Shoes Upper Materials of Fujian Province, Fujian Huafeng New Material Co., Ltd, Putian, 351164, China*

† Electronic supplementary information (ESI) available: TGA diagram, powder X-ray diffraction, CD, UV, *etc.* Crystal data and structure refinement details. CCDC 2062128–2062130. For ESI and crystallographic data in CIF or other electronic format see DOI: 10.1039/d1cc01249e

Firstly, the solvothermal reaction of $Zn(NO_3)_2$ and $KBH(bim)_3$ in a mixed DMF/ethanol/3-amino-1-propanol solution at 80 °C for 3 days led to an achiral 0D structure of cubic cages $Zn_4[BH(bim)_3]_4{\cdot}(NO_3)_4$ (BIF-26-Zn) (Fig. 1a and 2a);[37] while adding obb into this self-assembly system led to a chiral cage-based helix, BIF-109-Zn. BIF-26-Zn crystallized in the achiral space group $Pa\bar{3}$. The cubic cage of BIF-26-Zn was similar to the classical M_4L_4 cage mode, with four Zn(II) ions and four $BH(bim)_3^-$ ligands situated at the eight vertices of the cube (Fig. 1a). Interestingly, the crystallization of BIF-26-Zn occurred with the spontaneous resolution of $[BH(bim)_3]^-$ ligands into a pair of racemates, *S*-$[BH(bim)_3]^-$ and *R*-$[BH(bim)_3]^-$ (Fig. S1, ESI†). Even though each individual cubic cage is chiral, cages with opposite handedness (*SSSS*-$[Zn_4B_4]$ and *RRRR*-$[Zn_4B_4]$) coexist in the structure leading to an achiral crystal of BIF-26-Zn. In the cage, both the tetrahedral vertices (Zn and B) have C_3 symmetry, in which the fourth site of each Zn(II) center is just coordinated by a counter-anion or solvent offering opportunities for further linkage into the framework. Fortunately, when obb ligands were added into this assembly system, obb substituted a part of the coordination anions and occupied half of the open metal sites to connect these cages to form homochiral helical chains, BIF-109-Zn (Fig. 1b and c). Since the precursors are achiral, both enantiomeric pairs of BIF-109-Zn were observed in the bulk samples, which crystalized in the chiral space group $P3_121$ (*M*) or $P3_221$ (*P*), respectively. In BIF-109-Zn, obb ligands bridged adjacent Zn_4B_4 cages to form hexagonal shaped channels along the *c* axis, with the diameter of 11 Å and the screw-pitch of 8 Å. These helical channels packed with each other into a 3D superstructure (Fig. S2, ESI†). It is worth noting that all the helical channels are of the same handedness, and subsequently each individual crystal is chiral (Fig. 1d).

To gain a better insight into the relationship between chirality of molecular building blocks and helicity of crystal structures, we further analyzed the structure and found that both *SSSS*-$[Zn_4B_4]$ and *RRRR*-$[Zn_4B_4]$ cages exist in the same helical chain (Fig. S1, ESI†). Thus, the chirality of BIF-109-Zn comes from the absolute helical chains, whose formation is the result of highly distorted obb ligands with a dihedral angle between two central benzene rings of 74.8° (Fig. 1a). Possibly, the occurrence of spontaneous resolution of the chiral BIF-109-Zn should be attributed to the cooperative interactions between the twisted configuration of obb ligands and the homo-helical chain packing. The flexibility of the ligands played an important role in the chiral generation process. Additionally, to demonstrate the general applicability of this approach in the construction of helix, other crystals of BIF-110-Zn (Fig. S3, ESI†) with isostructural helical chains were synthesized by replacing the obb ligand in BIF-109 with another flexible 4,4′-carbonyldibenzoic acid ligand. By using this self-assembly synthetic strategy, the spontaneous resolution from achiral precursors to achiral crystal with enantiomeric cages then to chiral crystal with 1-D absolute helical chains can be realized.

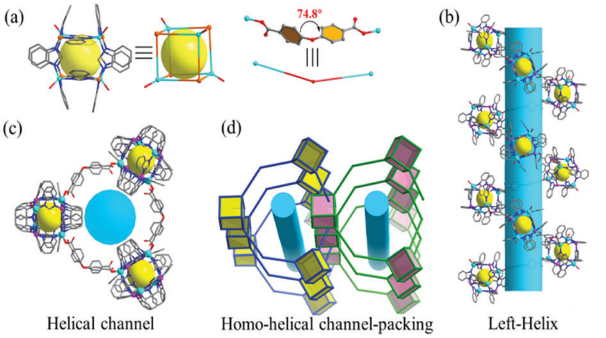

Fig. 1 Views of BIF-109-Zn (a) The building blocks of cubic cage BIF-26-Zn and obb linker in BIF-109-Zn; (b) big left-handed helix; (c) the helical channel along *c* axis; (d) the packing way between helical channels.

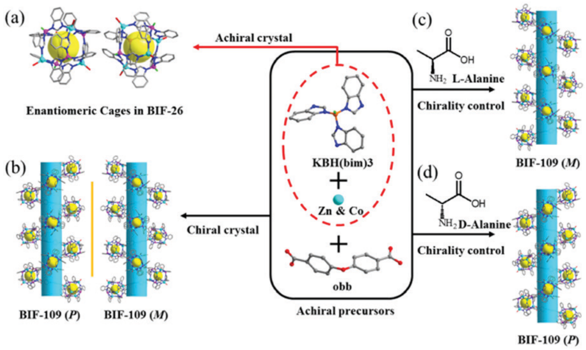

Fig. 2 Schematic representation of the generation of achiral crystals of BIF-26 (a), the mixture of BIF-109-Zn with opposite handedness (b), bulk homochirality of BIF-109-Zn (M) (c) and BIF-109-Zn (P) (d) induced by L-alanine and D-alanine from achiral precursors.

As mentioned above, the bulk sample of BIF-109-Zn is a mixture of crystals of opposite handedness as confirmed by single crystal X-ray diffraction analysis (Fig. 2b). Furthermore, the CD spectra indicate that the as-synthesized crystals are optically active, and an enantiomeric bias to favor one handedness is created during the crystallization process (Fig. S4, ESI†). However, the chiral orientation and the degree of enantiomeric excess are unpredictable. In order to obtain homochiral crystals and to further investigate the asymmetric induction crystallization, synthetic experiments were performed in the presence of various chiral induction agents. Indeed, a chirality induction effect was observed with L-alanine as the chiral catalyst and BIF-109-Zn (M) was prepared (Fig. 2c). The absolute configuration of BIF-109-Zn (M) was confirmed using single crystal X-ray diffraction data. The CD spectra of 10 randomly picked crystals from 4 separate synthetic batches with L-alanine consistently exhibit positive CD signals at 250 nm, suggesting that BIF-109-Zn (M) is the preferred configuration in the bulk sample (Fig. 3a). In contrast, replacing L-alanine with D-alanine induces the bulk samples of BIF-109-Zn (P) (Fig. 2d) which show opposite (negative) CD signals (Fig. 3b).

The phase purity of BIF-109-Zn and BIF-109-Zn (M) was confirmed by powder X-ray diffraction (PXRD) (Fig. S6 and S8, ESI†). Crystals of BIF-109-Zn (P) were too small to obtain the pure phase. The thermal gravimetric analysis (TGA, Fig. S10, ESI†) showed that BIF-109-Zn is stable up to 390 °C. Although the cage-based helical channels packed with each other, BIF-109-Zn still

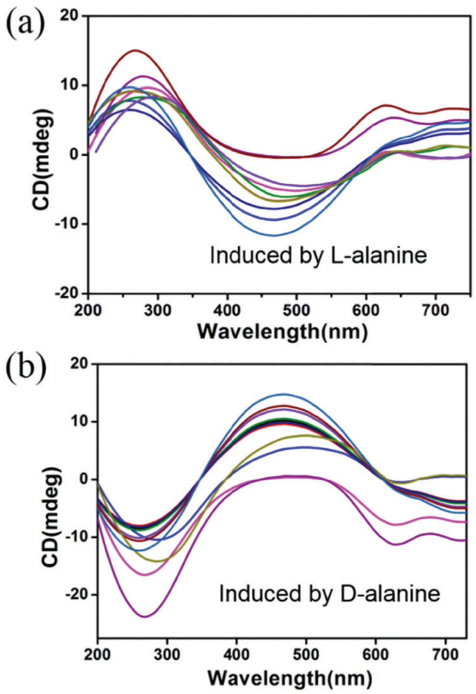

Fig. 3 The solid-state CD spectra of BIF-109-Zn (M) (a) and BIF-109-Zn (P) (b) prepared with L-alanine or D-alanine as chiral inducer.

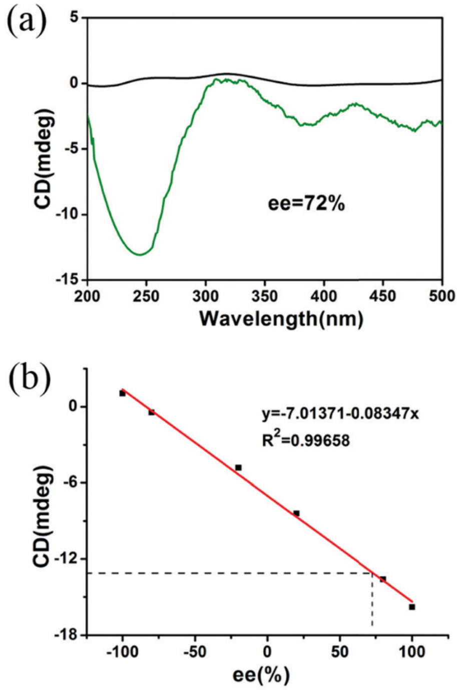

Fig. 4 (a) Enantioselective separation of racemic mixtures of 1-phenylethanol in ethanol solutions by BIF-109-Zn (M); (b) linear fits of CD signals at 250 nm in different ee%.

exhibited porosity with a solvent accessible volume of about 31.4% per unit cell estimated by PLATON. The permanent porosity of BIF-109-Zn was characterized by the CO_2 adsorption at 195 K, which showed type-I sorption isotherm with unusual hysteresis upon desorption (Fig. S12, ESI†). The CO_2 uptake value was 106.9 cm^3g^{-1} at 195 K, and the calculated Langmuir and Brunauer–Emmett–Teller (BET) surface areas were 513.9 m^2g^{-1} and 496.4 m^2g^{-1}, respectively. This low surface area may be due to the disordered counter-anions filled in these large voids.

To explore the potential of the absolute helical chains for chiral recognition, the bulk homochiral samples of BIF-109-Zn (M) were used for the enantioselective separation of racemic mixtures of 1-phenylethanol, and the circular dichroism (CD) signal of 1-phenylethanol was measured for monitoring the separation process. No CD signal was observed for the 1 : 1 mixtures of *R*-(+)-1- and *S*-(-)-1-phenylethanol (Fig. 4a), due to the offset of opposite cotton effects. The left-handed helical chains of BIF-109-Zn (M) were then added into this racemic mixture, and the supernatant was taken at intervals for CD measurement. The supernatant showed a negative cotton effect centered at 250 nm corresponding to the excess of *R*-1-phenylethanol (Fig. 4a), which indicates that the left-handed BIF-109-Zn (M) can capture and remove *S*-1-phenylethanol from the solution. After reaching adsorption saturation, the separation efficiency of BIF-109-Zn (M) for the racemic mixtures of 1-phenylethanol can be evaluated based on the calibration lines obtained from the CD intensities of standard solutions (Fig. 4b and Fig. S5, ESI†). The ee of BIF-109-Zn (M) was about 72%. PXRD showed that the recycled sample retained crystallinity after enantioselective separation (Fig. S9, ESI†). In addition, cycle tests revealed that BIF-109-Zn (M) could be reused without significant performance loss (Fig. S17, ESI†). This result demonstrated that the single-handed helical chains are indeed valuable for chiral recognition applications.

In summary, two cage-based boron imidazolate chains with absolute helicity were successfully synthesized in achiral reaction systems by mixing a C_3 symmetric rigid ligand, $KBH(bim)_3$, and a long flexible dicarboxylic acid ligand. The distortion of the long flexible ligands might control the connectivity between the cubic cages, and they become the driving force for linking the cages into helices and the spontaneous resolution of crystals. More importantly, the presence of proper chiral induction agents can selectively induce BIF-109-Zn (M) or BIF-109-Zn (P), making the helical orientation of bulk samples controllable. Notably, BIF-109-Zn (M) could be used for the enantioselective separation of racemic 1-phenylethanol with an ee value of 72%. This study reveals a novel strategy for the fabrication of 1-D absolute helix from achiral precursors and is useful for a better understanding of the homochirality in nature.

This work was supported by the National Natural Science Foundation of China (21773242, 21971241 and 21935010), and Strategic Priority Research Program of the Chinese Academy of Sciences (XDB20000000).

Conflicts of interest

There are no conflicts to declare.

Notes and references

1 C. Zhou, Y. Ren, J. Han, X. Gong, Z. Wei, J. Xie and R. Guo, *J. Am. Chem. Soc.*, 2018, **140**, 9417–9425.
2 M. Yoon, R. Srirambalaji and K. Kim, *Chem. Rev.*, 2012, **112**, 1196–1231.
3 J. Huang, L. Lin, D. Sun, H. Chen, D. Yang and Q. Li, *Chem. Soc. Rev.*, 2015, **44**, 6330–6374.
4 Z.-G. Gu, C. Zhan, J. Zhang and X. Bu, *Chem. Soc. Rev.*, 2016, **45**, 3122–3144.
5 W. Xuan, M. Zhang, Y. Liu, Z. Chen and Y. Cui, *J. Am. Chem. Soc.*, 2012, **134**, 6904–6907.
6 J. Zhang, S. Chen, A. Zingiryan and X. Bu, *J. Am. Chem. Soc.*, 2008, **130**, 17246–17247.
7 A. J. Alexander, *Cryst. Growth Des.*, 2008, **8**, 2631–2632.
8 M.-L. Ding, R. W. Flaig, H.-L. Jiang and O. M. Yaghi, *Chem. Soc. Rev.*, 2019, **48**, 2783–2828.
9 H.-X. Zhang, M. Liu, T. Wen and J. Zhang, *Coord. Chem. Rev.*, 2016, **307**, 255–266.
10 P. Horcajada, R. Gref, T. Baati, P. K. Allan, G. Maurin, P. Couvreur, G. Ferey, R. E. Morris and C. Serre, *Chem. Rev.*, 2012, **112**, 1232–1368.
11 H. Yang, F. Peng, C. Dang, Y. Wang, D. Hu, X. Zhao, P. Feng and X. Bu, *J. Am. Chem. Soc.*, 2019, **141**, 9808–9812.
12 Y. Cui, J. Zhang, H. He and G. Qian, *Chem. Soc. Rev.*, 2018, **47**, 5740–5785.
13 J.-P. Zhang, Y.-B. Zhang, J.-B. Lin and X.-M. Chen, *Chem. Rev.*, 2012, **112**, 1001–1033.
14 K. Sumida, D. L. Rogow, J. A. Mason, T. M. McDonald, E. D. Bloch, Z. R. Herm, T. H. Bae and J. R. Long, *Chem. Rev.*, 2012, **112**, 724–781.
15 J.-R. Li, J. Sculley and H.-C. Zhou, *Chem. Rev.*, 2012, **112**, 869–932.
16 J. Dong, Y. Liu and Y. Cui, *Acc. Chem. Res.*, 2021, **54**, 194–206.
17 S. Das, S. Xu, T. Ben and S. Qiu, *Angew. Chem., Int. Ed.*, 2018, **57**, 8629–8633.
18 F. Wang, Y.-H. Tang and J. Zhang, *Inorg. Chem.*, 2015, **54**, 11064–11066.
19 L. Ma, C. Abney and W. Lin, *Chem. Soc. Rev.*, 2009, **38**, 1248–1256.
20 J. Zhang, S. Chen, T. Wu, P. Feng and X. Bu, *J. Am. Chem. Soc.*, 2008, **130**, 12882–12883.
21 H. Zhu, Q. Li, B. Shi, H. Xing, Y. Sun, S. Lu, L. Shangguan, X. Li, F. Huang and P. J. Stang, *J. Am. Chem. Soc.*, 2020, **142**, 17340–17345.
22 S. A. Boer and D. R. Turner, *Chem. Commun.*, 2015, **51**, 17375–17378.
23 J. Zhang and X. Bu, *Chem. Commun.*, 2008, 1756–1758, DOI: 10.1039/b719368h.
24 M.-Y. Li, F. Wang and J. Zhang, *Cryst. Growth Des.*, 2020, **20**, 2866–2870.
25 C. Tan, X. Han, Z. Li, Y. Liu and Y. Cui, *J. Am. Chem. Soc.*, 2018, **140**, 16229–16236.
26 T. Kitao, Y. Nagasaka, M. Karasawa, T. Eguchi, N. Kimizuka, K. Ishii, T. Yamada and T. Uemura, *J. Am. Chem. Soc.*, 2019, **141**, 19565–19569.
27 J. D. Evans and F. X. Coudert, *J. Am. Chem. Soc.*, 2016, **138**, 6131–6134.
28 D. Wu, K. Zhou, J. Tian, C. Liu, F. Jiang, D. Yuan, J. Zhang, Q. Chen and M. Hong, *Angew. Chem., Int. Ed.*, 2021, **60**, 3087–3094.
29 L. Jiang, X.-L. Feng, C.-Y. Su, X.-M. Chen and T.-B. Lu, *Inorg. Chem.*, 2007, **46**, 2637–2644.
30 L. Xu, C. Qin, X. Wang, Y. Wei and E. Wang, *Inorg. Chem.*, 2003, **42**, 7342–7344.
31 X. Zhao, M. S. Shimazu, X. Chen, X. Bu and P. Feng, *Angew. Chem., Int. Ed.*, 2018, **57**, 6208–6211.
32 Z.-X. Xu, Y.-X. Tan, H.-R. Fu, Y. Kang and J. Zhang, *Chem. Commun.*, 2015, **51**, 2565–2568.
33 X. Huang, Q. Li, X. Xiao, S. Jia, Y. Li, Z. Duan, L. Bai, Z. Yuan, L. Li, Z. Lin and Y. Zhao, *Inorg. Chem.*, 2018, **57**, 6210–6213.
34 X. Luo, Y. Cao, T. Wang, G. Li, J. Li, Y. Yang, Z. Xu, J. Zhang, Q. Huo, Y. Liu and M. Eddaoudi, *J. Am. Chem. Soc.*, 2016, **138**, 786–789.
35 J. Zhang and X. Bu, *Chem. Commun.*, 2009, 206–208.
36 Z. Yang, J. Shang, Y. He, Y. Qiao, P. Ma, J. Niu and J. Wang, *Inorg. Chem.*, 2020, **59**, 1967–1972.
37 T. Wen and J. Zhang, *Inorg. Chim. Acta*, 2017, **460**, 89–92.